Flame Emission Spectroscopy: Fundamentals and Applications[†]

Giorgio Zizak

CNR-TeMPE, Istituto per la Tecnologia dei Materiali e dei Processi Energetici
Via Cozzi 53, 20125 Milano, Italy

Introductory Remarks

Classification of Emission Spectra
- *Continuous spectra*
- *Discontinuous spectra*

Emission Spectra of Flames
- *Hydrogen flames*
- *Hydrocarbon flames*

Origin of Spectra
- *Formation of excited OH**
- *Formation of excited CH* and* C_2*
- *Formation of* CO_2*

Intensity of the Emission Lines

Some Emission Spectra in the UV-VIS
- *OH* spectrum*
- *CH* spectrum*
- C_2* *spectrum*

Flame Temperature Measurements
- *Thermodynamic equilibrium in flames*
- *Temperature measurements by emission spectroscopy techniques*
- *The Line Reversal method*

Industrial Combustion Monitoring and Control
- *UV-VIS emission spectroscopy and tomography*
- *Air-ratio determination and control in a gas boiler*

[†] Lecture given at the ICS Training Course on Laser Diagnostics of Combustion Processes, NILES, University of Cairo, Egypt, 18-22 Nov. 2000

Introductory Remarks

When energy is supplied to a body in particular forms such as heat or electrical discharges, the body restores part of this energy in the form of electromagnetic radiation. Spectral analysis consists of sorting this radiation in function of its wavelength, this distribution being called an emission spectrum. The radiation can fall into the visible domain (such as the yellow sodium light or the blue mercury emission) or it can be comprised in the infrared and ultraviolet domains.

It is hardly possible to give a description of the spontaneous emission of flames that will be valid generally because the radiation is not only sensitive to temperature, varying with wavelength and the kind of gas mixture, but also depends on many other factors which include the gas/air or gas/oxygen mixture ratio, the gas purity, the burner type, the gas flow (laminar or turbulent), the presence of sprayed additives and the height of observation in the flame. The appearance of a recorded flame spectrum is also affected by the resolving power of the spectrometer. When large slit widths are used the detailed structure of the spectrum is smeared out and molecular bands look more like continua (quasi-continua).

Emission techniques when applied to flames can provide valuable insights into many flame processes. This is important in a variety of contexts, but it must always be remembered that emission techniques, when applied in the ultraviolet and visible part of the spectrum, are of peripheral interest for the analysis of major flame processes. In fact in these spectral regions the emissions are chemiluminescent and stem from minor side reactions requiring radical-radical reactions to provide sufficient energy to radiate. Nonetheless there have been many interesting studies of the structure of the flame emissions and there is a substantial body of literature. Moreover emission spectroscopy techniques are line-of-sight techniques and different parts of the flame such as the primary and secondary combustion zones and the interzonal region, are observed. These radiation components are difficult to be separated and the observed spectrum can be difficult to be interpreted.

Therefore some caution should be used in applying emission spectroscopy for flame diagnostics, but properly applied the techniques can be quite useful.

The topics covered in this lecture reflect the author’s interests and are not exhaustive of all the applications of emission spectroscopy techniques in flames. In particular the emission spectroscopy in the infrared with the important area of the FT-IR technique will not be covered in this survey. Similarly the subject of atomic flame emission spectroscopy for analytical applications will not be treated. In this lecture flame emission mainly in the UV-VIS part of the spectrum will be described in some detail and applications regarding flame temperature measurements and industrial combustion monitoring will be presented

Classification of Emission Spectra

Experience shows that the energy distribution (or spectrum) the spontaneous emission from flames can be classified according to different shapes. Thus the following types of spectra can be distinguished:

Continuous spectra, such as the ones radiated by the sun, in which the emitted energy is distributed in a continuous manner between all wavelengths within a certain domain, and which usually exhibits a maximum. This is the general case of radiation emitted by heated bodies in solid or liquid phase. Continuous spectra in combustion systems are generally observed in the sooty region of rich hydrocarbon flames. In some cases the continuous emission in flames may be due to processes such as recombination of ions, or associations of atoms and radicals.

Discontinuous spectra, in which the energy is mainly confined around certain narrow wavelengths: these types of spectra are attributed to isolated atoms or molecules. In this Lecture we will be concerned mostly with this category of spectra. An examination, even superficial, of discontinuous spectra shows that they can be classified into two categories, as shown in figures 1 and 2.

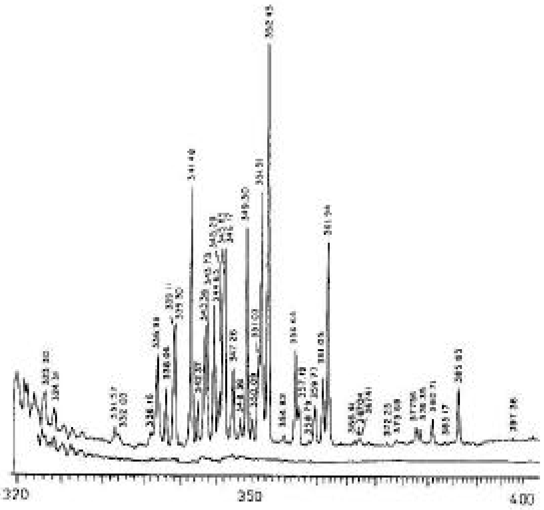

Figure 1. Nickel spectrum in oxyhydrogen flame (from Alkemade, 1979)

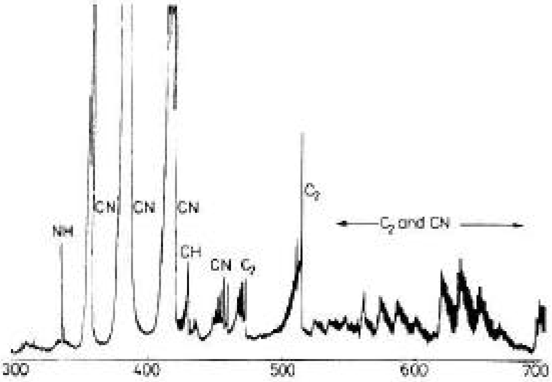

Figure 2. Spectrum of a fuel-rich nitrous oxide-acetylene flame (from Alkemade, 1979)

In the first figure most of the spectrum is composed by **isolated lines** arranged without any order except in some rare cases. This assembly of spectral lines constitutes a **line spectrum.** These line spectra are attributed to free atoms, and hence they are named **atomic spectra.** In the second figure the lines are arranged in groups, each group being called a **band**. The name **band spectra** is thus given to spectra presenting such a characteristic aspect. In general one edge of the band, the band head, is sharp; the other edge is not and the band intensity is degrading, either toward the longer wavelengths or toward the shorter. Sometimes it happens that a band head of another band is superimposed. These band spectra are attributed to free molecules and they are called **molecular spectra**.

Emission Spectra of Flames

Spectra in the visible and ultra-violet regions are generally due to changes of electronic energy, i.e. to a transition from one configuration of electrons of the molecule to another configuration. This change determines the position of the band system as a whole. Accompanying changes in the vibrational energy of the atoms of the molecule determine the position of individual bands within the band system. Accompanying changes of rotational energy of the molecule as a whole determine the fine structure of individual bands, i.e. the fine line structure of the band.

None of the ordinary molecules which are the stable products of combustion, such as H_2O, CO_2, CO, O_2, or N_2 possesses electronic energy levels situated so as to enable these molecules to give spectra of appreciable strength in the visible or ultraviolet regions. The only product of combustion which has an appreciable equilibrium concentration which does give a strong spectrum in this spectral region is the hydroxyl radical OH, which gives a band system with the strongest head at 306.4 nm. The spectrum of OH will be described further on.

In the reaction zone of flames, corresponding to the inner cone of the Bunsen flame, many unstable radicals such as CH, C_2, HCO, NH, NH_2 etc. may be formed and these do give appreciable emission in the visible and near ultraviolet. The spectra of some of these molecules (CH and C2) will be described in the following paragraphs.

In the infrared region of the spectrum (figures 3, 4 and 5) H_2O has strong vibrational bands at 1.8, 2.7 and 6.3 μ and a rotational band that covers the region from 10 to about 100 μ. CO_2 emits at 2.8, 4.3 and 15 μ. Other vibrational bands of interest are CO at 2.3 and 4.5 μ, NO at 2.6 and 5.2 μ and the OH vibrational bands that cover the near infrared area to about 4 μ.

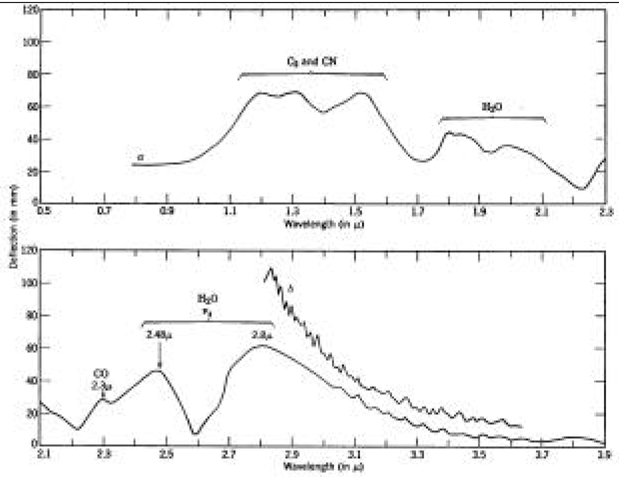

Figure 3. Infrared emission of the oxyacetylene welding torch flame. a) reaction zone. b) post reaction zone (from Mavrodineanu and Boiteux, 1965)

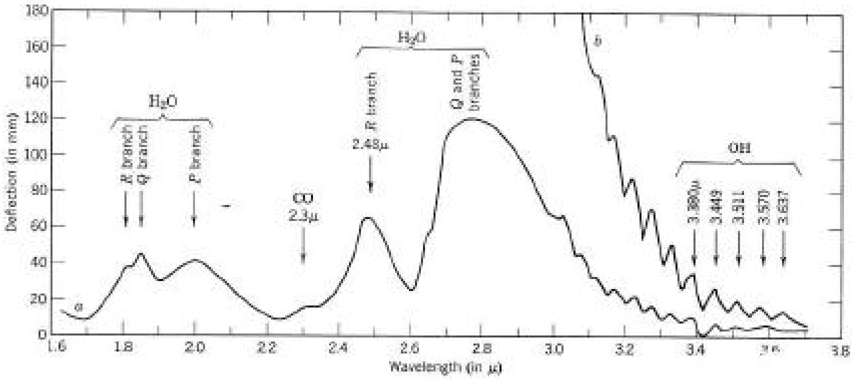

Figure 4. Emission spectrum of the oxyacetylene welding torch a) oxygen content greater than the conditions of fig.3. b) maximum oxygen content. (from Mavrodineanu and Boiteux, 1965)

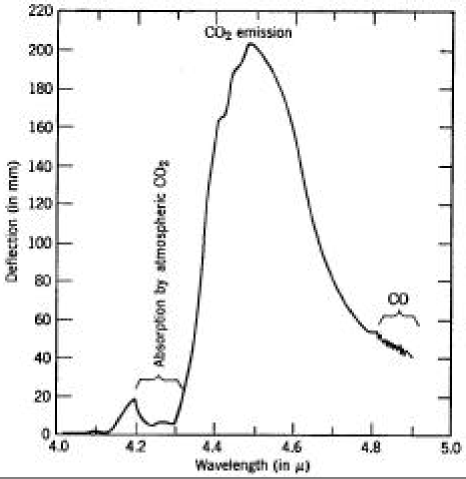

Figure 5. Emission spectrum of the oxyacetylene flame between 4.1 and 4.9 μ, showing absorption and emission of CO_2 (from Mavrodineanu and Boiteux, 1965).

It follows from the Wien's displacement law that at flame temperatures the maximum emission will tend to be in the near infrared between about 2μ and 1 μ according to the temperature of the flame. For clean flames the radiation in the visible and ultraviolet accounts usually for less than 0.4 % of the heat of combustion. This visible radiation comes mainly from the inner cone, while the infrared radiation comes from the main body of the gases, both interconal gases and burnt products. For luminous flames, radiation from hot carbon particles will increase the radiation in the visible with a spectrum that resembles the continuous spectrum of a black body.

Hydrogen flames

Compared with other flames the hydrogen flames, including the nitrous oxide-hydrogen flames, have the characteristic of a weak background emission. The spectra (figure 6) always show the marked OH bands with band heads at 281 nm, 306 nm (strong) and 343 nm.

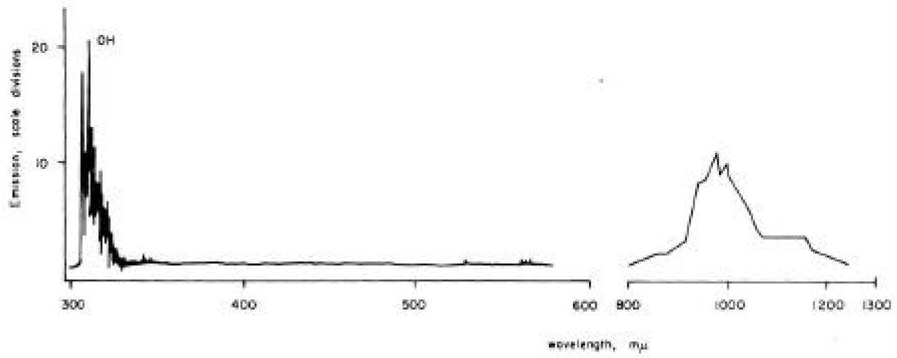

Figure 6. Spectrum of oxygen-hydrogen flame (from Pungor and Cornides, 1969)

The hotter oxyhydrogen flames also emit the Schumann-Runge O_2 bands between 250 nm and 400 nm, and a weak continuum in the blue and ultraviolet regions of the spectrum. This continuum, which in the absence of impurities practically does not exist in the spectrum of air-hydrogen flames, is attributed to the recombination of OH and H to H_2O. When, on addition of nitrogen compounds, free NO radicals exist in the flame, NO bands appear in the ultraviolet and a green (quasi-) continuum can also result from the recombination of NO and O to NO_2. The intensity of the O_2 bands can be appreciably reduced by feeding a slight fuel-gas excess into the hydrogen flame. In the infrared region the strong vibration-rotation bands of H_2O at 0.9-1.1 μ and at 1.8-3.0 μ appear; with oxyhydrogen flames weak wings of these bands extending into the red end of the visible spectrum. The background emission from the primary combustion zone does not substantially differ from the emission of the other parts of the flame. In the nitrous oxide-hydrogen flames the radiation from the region above the primary combustion zone presents the bands of OH and NO (between 220 nm and 280 nm) and NH (at 336 nm and 337 nm) and further a (quasi-)continuum (from 350 nm to 600 nm) which is attributed partially to the recombination of NO and O. From the combustion zone an emission of the NH_2 band additionally appears in the visible spectral region.

Hydrocarbon flames

Much more complex are the spectra of hydrocarbon flames, for example oxyacetylene flames, which not only produce the bands and the continua observed in hydrogen flames, but also emit radiation of hydrocarbon radicals.

From the region above the primary combustion zone, the radiation contains, besides the above mentioned OH bands, another fairly strong component which with a spectrometer of only moderate resolving power appears as a quasi-continuum. This is normally attributed to the emission from excited CO_2. The spectrum extends from below 300 nm to 600 nm and gives the flame the well known blue color. With flames burning with excess fuel in the free atmosphere this blue radiation and the ultraviolet OH bands are observed mainly in the emission from the outer zone of the flame in which the secondary combustion takes place. Also weak violet CN bands are found in air-acetylene flames, the intensity of which diminish with increasing distance from the combustion zone. The oxyacetylene flames produce the O_2 bands mentioned above, and some CO bands between 205 nm and 245 nm. In the infrared, apart from the H_2O bands, there is the appearance of some strong vibration-rotation bands of CO_2 around 2.8 μ and 4.4 μ, and several CO bands at 2.3-2.8 μ. If the primary oxygen supply is insufficient, the H_2O and CO_2 bands are mainly due to emission from the outer flame zone.

The primary combustion zone of hydrocarbon flames is distinct from the other parts of the flame by its emission of mostly visible bands (figure 7), namely CH bands at 387/9 nm and 432 nm and C_2 bands between 436nm and 563 nm (the so called Swan bands). These bands may also be emitted by the region above the primary combustion zone with a very fuel-rich gas mixture. Furthermore, the ultraviolet OH and CO radiation from the combustion zone are stronger than those from the zone above it. In the cooler flames it is possible to detect the Vaidya bands of the CHO radical between 300 nm and 400 nm. With an excess of fuel the atomic carbon line at 247.8 nm also appears. If there is a considerable oxygen deficiency or if substances such as aromatic compounds are sprayed, the flame becomes white luminous as a result of the thermal continuous emission of unburnt soot particles.

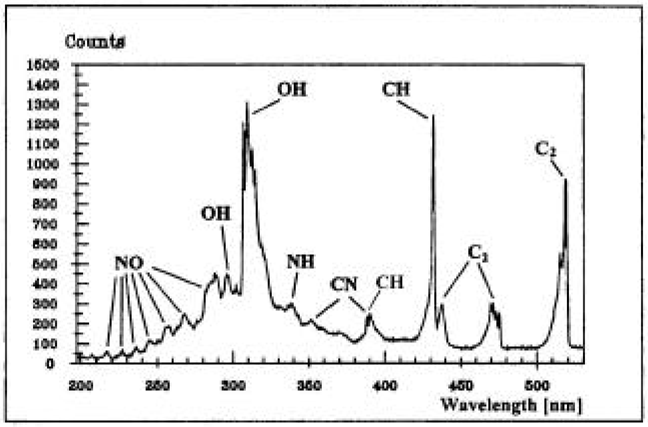

Figure 7. Emission spectrum of a rich premixed butane-air flame (adapted from Obertacke, 1996).

In the spectrum of the primary combustion zone as well as of the red-violet interconal zone of fuel-rich nitrous oxide-acetylene flames the bands of CN, C_2, CH and NH can be detected between 300 nm and 700 nm (figure 2).

Origin of Spectra.

The emission of the primary combustion zone especially and, to some degree, of the flame region above it, cannot be described in terms of thermal equilibrium. Hence, for a quantitative interpretation of the flame emissions, not only the concentrations of the emitting molecules and the flame temperature, but also the various formation and excitation mechanisms have to be known. In spite of diverse comprehensive investigations, these mechanisms are not yet entirely clear. Moreover the probability of quenching collisions between the superthermally excited species and the gas molecules as well as the possibility of self-absorption must be taken into account. An additional difficulty in dealing with the primary combustion zone arises from the very pronounced spatial variations of the gas composition.

Most of the investigations in this field were undertaken with the direct purpose of understanding the combustion reactions or the structure of the radiating molecule instead of explaining the background emission of flames. These investigations were carried out under particular experimental conditions, such as flames of low temperature burning at low pressure, discharge tubes, explosions and shock waves. Therefore the results obtained in this way can not be always applied to flames. In spite of these difficulties, there is a general agreement about the following excitation mechanisms (Wohl *et alii*, 1955; Gaydon, 1957, Porter *et alii*, 1966; Guillaume, *et alii*, 1984, Najim, *et alii*, 1998).

Formation of excited OH. Excited OH radical, OH*, can be formed in the primary combustion zone by the following chemiluminescent reaction:

$CH + O_2 \rightarrow CO + OH^*$

Other possible reactions, also of importance for hydrogen flames, are:

$O + H \rightarrow OH^*$
$H + O_2 \rightarrow OH^* + O$

Here also intermediate excited states or complexes can occur. Furthermore, an OH radical can be raised from the ground state into the excited state when it is involved as a third partner in a recombination reaction between two other particles such as:

$OH + (O)H + H \rightarrow OH^* + H_2O$

This reaction explains why the presence oh H and OH radical in hydrogen and acetylene flames in excess of their equilibrium concentration also leads to a superthermal excitation of the OH band above the primary combustion zone.

Formation of excited CH and C_2 . The formation of excited CH and C_2 (d $^3\Pi_g$), CH* and C_2*, in flames has been debated for long time. Comparison of CH* emission from various flames leads to the conclusion that CH* is not formed by direct beakdown of acetylene but by a side reaction. The observation that CH* (A $^2\Delta$ or B $^2\Sigma^-$) usually occurs higher in the reaction zone than C_2 suggests that it might be formed from C_2 by the reactions:

$C_2 + OH \rightarrow CO + CH^*$
$C_2H + O \rightarrow CO + CH^*$

which are very exothermic and sufficient to bring CH up to A and B states.

Concerning the formation of C2* most of the studies favor the reactions:

$CH_2 + C \rightarrow H_2 + C_2^*$
$CH + C \rightarrow H + C_2^*$

Formation of excited CO_2. The origin as well as the structure of the so-called “blue continuum” radiation of carbon monoxide and hydrocarbon flames have been much debated. According to recent investigations this blue continuum is not given by simple recombination reactions. It is possible to show that the flame radiation is not really a continuum, but has rotational fine structure which is smeared out at only moderate spectral resolution. The origin of the emission is given by the following three-body collision:

$^1CO + {}^3O + X \rightarrow {}^3CO_2^* + X$

where X is a flame molecule, ^1CO denotes a CO molecule in the singlet state, ^3O is an O atom in the triplet ground state and $^3CO_2^*$ a CO_2 molecule in an excited triplet state. The third partner X acts as a stabilizer of the newly formed CO_2 molecule. This molecule then goes over, without radiating, into a neighbouring excited singlet state ($^1CO_2^*$) from which it can make an allowed radiative transition to the electronic singlet ground state

$$^1CO_2^* \rightarrow {}^1CO_2 + h\nu$$

In this transition since the initial and the ground states are stable the frequency ν of the emitted photon can only have discrete values and the resulting spectrum will have a discrete structure. The expected complexity of the spectrum however may explain why at low resolution and high temperature the spectrum appears as a quasi-continuum. As a result of a quenching collision with a flame molecule $^1CO_2^*$ can also pass radiationless into the ground state

$$^1CO_2^* + X \rightarrow {}^1CO_2 + X,$$

while X will take up the released excitation energy. As all processes are basically reversible the reverse transition is also possible and is described by the above reaction with the arrow pointing in the opposite direction. Excited $^1CO_2^*$ molecules can thus be formed in two ways: either through recombination of one CO molecule and one O atom; or through collisional excitation of a CO_2 molecule in the ground state by an X molecule.

Intensity of emission lines

The intensity relations of the lines in a spectrum are of greatest importance for practical spectroscopy. In fact a quantitative analysis of the spectra is based on the existence of a definite relationship between the concentration of atoms or molecules, to be determined, and the intensity of a specific radiation. Several phenomena have a play in the measured intensity. In the following paragraph the basic concepts involved and the relationships necessary for the interpretation of the emission lines will be given.

According to Bohr's theory, energy is emitted when a transition occurs from one energy level, n, to another energy level, m, of an atom or a molecule, $E_n \rightarrow E_m$. As the energy emitted in any transition is the light quantum $h\nu$, the intensity I_{em} of a spectral line emitted at the frequency ν may be calculated from the number of atoms (molecules) undergoing the transition n to m in the time interval dt:

$$dN_{nm} = A_{nm} N_n \, dt$$

where N_n is the population of the initial state and the proportionality coefficient A_{nm} is the Einstein transition probability of spontaneous emission. The emission intensity is then given by:

$$I_{em} = A_{nm} N_n h\nu$$

where h is the Planck constant. Photons are emitted isotropically in all directions, and only a fraction $d\Omega/4\pi$ is received, if $d\Omega$ is the solid angle subtending the aperture of the receiving optics. In the presence of an external radiation at the same frequency ν, transitions in the opposite direction (absorption) can also take place. The number of absorption transitions may be expressed by the equation:

$$dN_{mn} = B_{mn}\, \rho(\nu)\, N_m\, dt$$

where $\rho(\nu)$ is the spectral volume density of the radiation, N_m is the population of the lower state m, and B_{mn} is the Einstein transition probability of absorption. In producing new excited states, the absorption of radiation gives rise to induced or stimulated emissions. The number of corresponding transitions may be expressed by:

$$dN^*_{nm} = B_{nm}\, \rho(\nu)\, N_n\, dt$$

where B_{nm} is the Einstein transition probability of induced emission. At equilibrium the principle of microscopic reversibility holds:

$$dN_{nm} + dN^*_{nm} = dN_{mn}$$

and therefore:

$$[A_{nm} + B_{nm}\, \rho(\nu)]\, N_{nm} = B_{mn}\, \rho(\nu)\, N_{mn}$$

The three Einstein coefficients are related by the expressions:

$$B_{nm} = (g_m/g_n)\, B_{mn}$$

and

$$A_{nm} = (8\pi h\nu^3/c^3)\, B_{nm}$$

Where g_m and g_n are the statistical weights of the states m and n, and c is the speed of light. The A_{nm} coefficient is related to the classical oscillator strength, f_{nm} , and the “strength”, $S_{\mathbf{nm}}$ of the transition by the relations:

$$A_{nm} = (8\, \pi^2\, e^2/\lambda^2 mc)\, f_{nm} = (64\, \pi^4\, \nu^3\, /3hc^3\,)\, S_{nm}\, /g_n$$

where e and m are the electron charge and mass respectively. The intensity emitted by unit volume is therefore given by:

$$I_{em} = (8\pi^2 e^2 h/m\lambda^3)\, N_n\, f_{nm}$$

Emission and absorption lines are never widthless, as implicitly assumed. They are spread over a definite range of wavelengths or frequencies with a maximum at a certain wavelength λ_0 or frequency ν_0 , as indicated in fig.8. The number of atoms (molecules) involved in transitions giving a radiation in the frequency range ν, $\nu+d\nu$ is only a fraction, δN_n or δN_m , of the total population of levels n and m. In emission flame spectrometry however, the resolving power of the instrument is not, in general, sufficient to resolve the shape of the lines and the observed intensity is the integral over the spectral region where the emission is different to zero. The measured signals are then given by:

$$I_{em} = \int I_{em}(\nu)\, d\nu$$

For absorption measurements an absorption coefficient $k(\nu)\, d\nu$ is defined such as:

$$k(\nu)\, d\nu = h\nu/c\, (B_{mn}\, \delta N_m - B_{nm}\, \delta N_n)$$

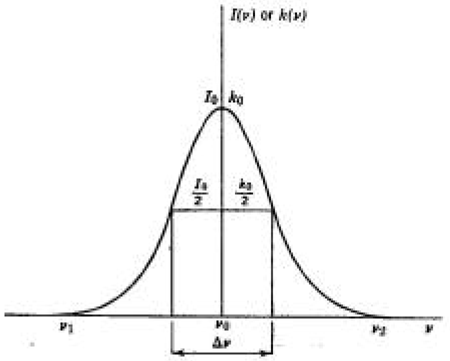

Figure 8. Shape of an emission or absorption line (arbitrary).

The integrated absorption K is then given by:

$$K = \int k(\nu)\, d\nu = h\nu/c\ (B_{mn} N_m - B_{nm} N_n)$$

In flames the ratio N_n/N_m is always very small and absorption is practically restricted to lines involving the ground state. In this case the integrated absorption is given by:

$$K = (\lambda_0^2 / 8\pi)\ A\ (g_1/g_0)\ N_0$$

In which N_0 is the number concentration of species in the ground state, g_0 and g_1 are the statistical weight of the levels involved in the absorption process and A is the transition probability of the line.

Moreover the intensity emitted by a flame is the integral of the intensities emitted along the observation path. Some of the photons can be absorbed inside the flame and consequently the beam emitted at a given point is weakened during its travel toward the edge of the flame. Considering a uniform slab of flame limited by two parallel planes P_1 and P_2 (fig. 9) at abscissas *0* and *l*, perpendicular to the line of sight *0x*; a small volume of width *dx* and unit section, located at *x*, contains N_1 *dx* atoms (molecules) excited in the level E_1; in the direction of the observer *Ox'* it emits an intensity

$$dI' = I_{em}\ \alpha\ dx$$

where α is a constant factor depending only on the measuring instrument. In travelling from *M* to *O* toward the observer, this intensity is reduced by absorption and becomes:

$$dI = dI' \exp(-Kx)$$

where K is the integrated absorption, previously defined. The received intensity, I, is the sum of all the intensities dI emitted by all small volumes of the flame from *x*=0 to *x*=*l*

$$I = \int dI = \alpha\ (I_{em}/K)\ [1 - \exp(-Kl)]$$

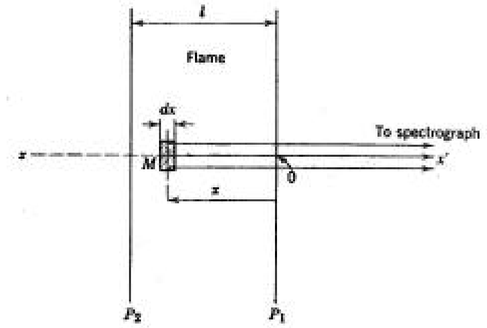

Figure 9. Column of flame, with the path of a beam emitted by a small volume at distance *x* from the front plane P_1 (from Mavrodineanu and Boiteux 1965).

By using the previous formula for K and I_{em}, the measured intensity of the line is given by the expression:

$$I = \alpha \, (8\pi hc/\lambda^3) \, (N_1/N_0) \, (g_0/g_1) \, \{1\text{-}\exp[- (\pi e^2/mc) \, N_0 \, f \, l]\}$$

This equation shows that the measured intensity depends on *l* through an increasing exponential term; for small values of *l*, the integrated intensity, I, is proportional to it:

$$I = \alpha \, I_{em} \, l$$

This relation is exactly what would be obtained by neglecting the absorption. The same result is obtained when K is very low, as it is when the lower level of the transition is an excited state; this justify the neglect of self-absorption for radiation other than the one starting from the ground state.

Some emission spectra in the UV-VIS

OH spectrum. The existence of the OH molecule in flames and in many other laboratory or natural sources, is proven through the ultraviolet bands with a widely open structure, the strongest of which lies at λ 306.4 nm. Due to the importance of OH in the kinetics of flames and related problems, the ultraviolet bands have extensively and thoroughly studied. The lower state of the ultraviolet band, which is the ground state of OH, is an inverted doublet Π state, the component $^2\Pi_{1/2}$ lying above $^2\Pi_{3/2}$. The higher state is a normal doublet Σ state noted $A^2\Sigma^+$. Figure 10 represents the first vibrational levels of the two involved electronic states with indication of the energy levels, in electron volts, measured from the vibrational state v=0 of the $X^2\Pi$ state.

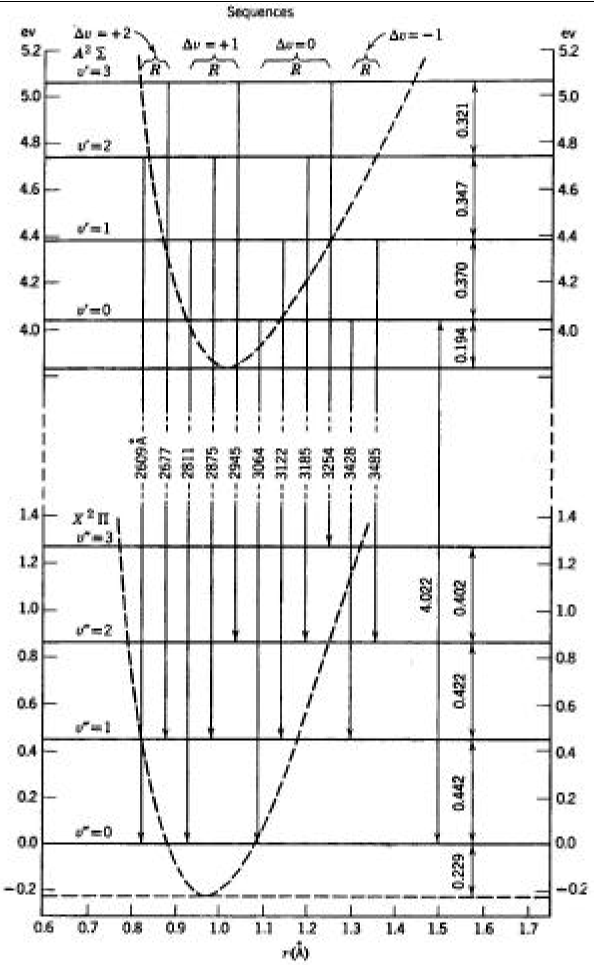

Figure 10. Vibrational energy levels diagram of the A $^2\Sigma$ and X $^2\Pi$ states, and transition of the OH molecule with Morse potential curves (from Mavrodineanu and Boiteux, 1965).

The spin doubling is too small to be represented. Every band is represented by a vertical line connecting the involved vibrational levels. The most intense band is the (0,0) band at 306.4 nm. Fig. 11 shows the rotational structure of this band as observed at medium resolution in a methane-air flame. It should be pointed out that there are two other bands systems attributed to OH. One ($B^2\Sigma^+$-$A^2\Sigma^+$) is located in the visible from 420 nm to 600 nm, the other ($C^2\Sigma^+$-$A^2\Sigma^+$) is located in the ultraviolet from 224.8 nm and 260.0 nm. These bands have been observed in discharges through water vapor but have never been identified in flames and therefore they are of no interest for combustion diagnostics.

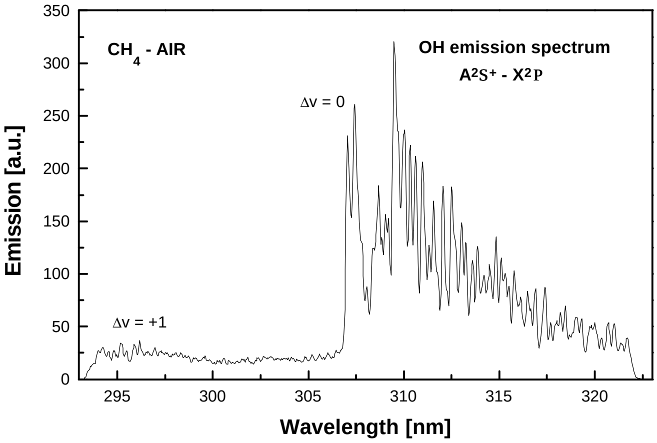

Figure 11. OH spectrum in a lean premixed methane-air flame.

CH spectrum. Three band systems ascribed to the CH molecule are emitted by the inner cone of the hydrocarbon flames; the strongest one is around λ 431.5 nm, another one is between λ 362.8 and 420.0 nm, the last band is in the ultraviolet near λ 315.0 nm. Fig. 12 shows an energy diagram with all the observed bands of CH*. In flames are particularly visible the (0,0) band of the B $^2\Sigma^-$-X $^2\Pi$ system at 387.2 nm and the strong blue-violet spectrum of the A $^2\Delta$-X $^2\Pi$ system. Part of this spectrum is shown in fig. 13 at medium resolution. This system is often referred as the 431.5 nm system. It consists mainly of a violet-degrading band with two Q heads at 431.25 and 431.50 nm that can not be separated in usual conditions. A strong overlap by the C_2 Swan band ($\Delta v = 2$) obscures the P lines and at 432.4 nm a “strong” line is observed which consists of a piling up of Q lines of the (2,2) band. The other $B^2\Sigma^-$ - $X^2\Pi$ system is in the near ultraviolet with strong R and Q band with heads at 387.2 nm and 388.9 nm respectively. Finally the ultraviolet system ($C^2\Sigma^+$ - $X^2\Pi$) has the characteristic that the head of the Q lines of the (0,0) band emerges at 314.4 nm among the OH ultraviolet lines. Another “line” may be seen at 315.7 nm and is the head of the (1,1) band.

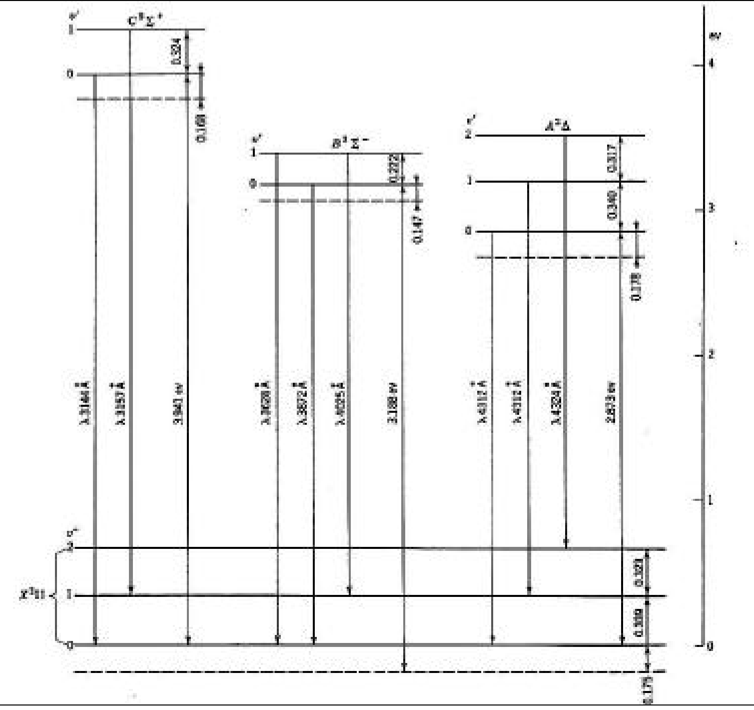

Figure 12. Vibrational energy levels diagram and transition of CH molecule (from Mavrodineanu and Boiteux, 1965)

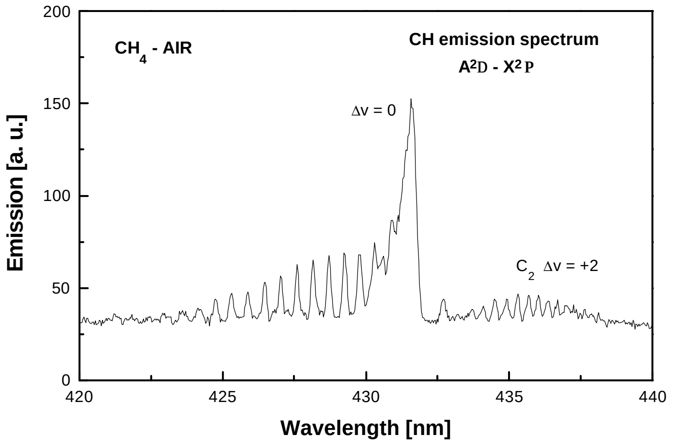

Figure 13. CH emission spectrum in a lean premixed methane-air flame.

C_2 spectrum. There are seven known band systems attributed to the C_2 molecule. Fig. 14 reports the energy levels diagram and transitions of this molecule (note: the energy labeling is the old one in which the $^3\Pi_u$ level is considered the lowest one instead of the singlet $^1\Sigma_g^+$. The capital letters are then given to the triplets levels). These systems result from transitions between triplet levels or between singlet levels, but no intercombination systems connecting triplet and singlet levels are known.

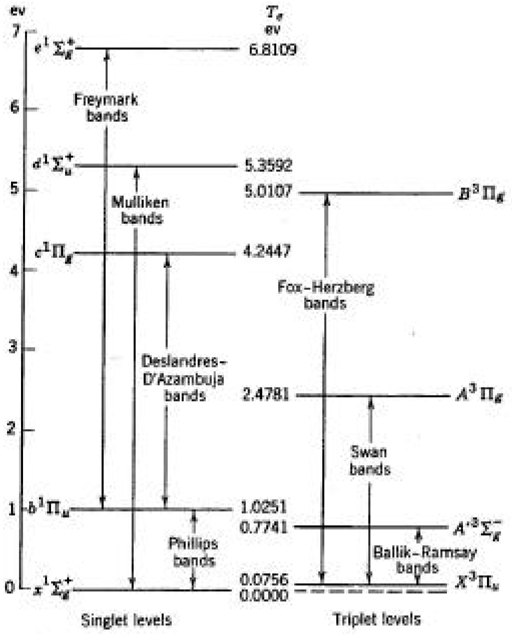

Figure 14. Energy levels diagram and transitions of C_2 molecule. Each electronic state is represented by its lowest vibrational level (from Mavrodineanu and Boiteux, 1965).

On the triplet side the observed bands belong to the:

Fox-Herzberg system between 237.8 nm and 300. 0 nm,
Swan system between 435.0 and 686.0 nm
Balik-Ramsey system, lying in the infrared around 1765.7 nm and degrading toward the long wavelengths

On the singlet side the bands belong to the:

Freymark system in the ultraviolet at 214.3 nm,
Mulliken system in the ultraviolet around 231.26 nm,
Deslandres-D'Azambuja system with bands degrading toward shorter wavelenghts between 358.0 nm and 386.0 nm,
Phillips system with bands degrading towards longer wavelengths and lying in the infrared at 1209.1 nm

Although all these bands can be observed in the inner cone of acetylene flames, the most characteristic features of C_2 in all hydrocarbon flames are the Swan bands, which give the

characteristic blue-green color. Fig. 15 shows the Δ*v*=+1, 0, and –1 bands in low resolution as detected in a methane-air flame superimposed to the blue continuum of CO_2*. The bands are degrading toward the violet with prominent band heads of the
(0,0), (1,1), (1,0), (2,1) etc. sequences.

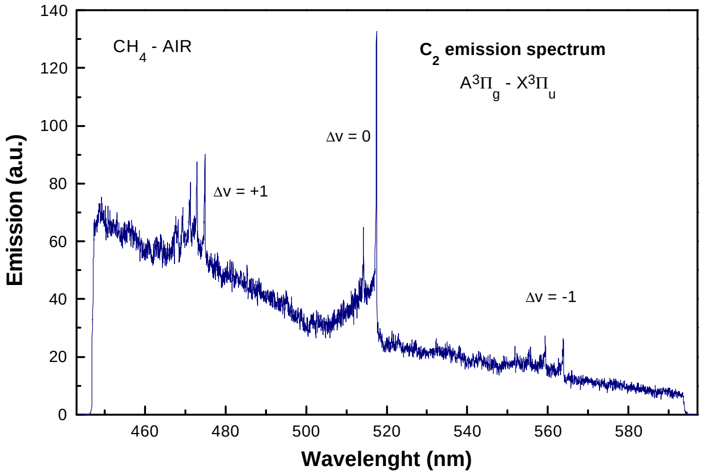

Figure 15. Low resolution spectrum of C_2 in a lean premixed methane-air flame

Flame temperature measurements by emission techniques

Thermodynamic equilibrium in flames. The concept of temperature is rigidly derived in thermodynamics. It is possible to set up a temperature scale which is based upon a Carnot cycle. In the kinetic theory of gases the temperature has been introduced as a quantity proportional to the mean translational energy of the particles; this concept yields to the perfect gas temperature scale. Also, the theory of the black body radiation can be used to develop a temperature scale according to Planck's radiation formula. It has been shown that the latter temperature scales are equivalent to the thermodynamic scale.

The assumption underlying the assignment of a temperature to a system is that the system is in a state of thermodynamic equilibrium. Such a state can be characterized by the fact that it satisfies a number of conditions with the use of a single value of the quantity T, which then represents the temperature of the system. For a gaseous system these conditions are:

1) A velocity distribution of the particles according to the Maxwell equation:

$$f(v)\, dv = 4\pi\, (m/2\pi kT)^{3/2}\, v^2 \exp(-mv^2/2kT)\, dv$$

where $f(v)\, dv$ is the fraction of the particles with velocities between v and v+dv, m is the mass of the particles and k is the Boltzmann constant

2) A population of the atomic and molecular energy levels according to the (simplified) Boltzmann formula:

$$N_i/N_0 = (g_i /Q) \exp(-E_i/kT)$$

Where N_0 is the total number of a kind of particles, Q is the partition function, g_i is the statistical weight of level i and E_i is the energy of the level.

3) An ionization of a kind of atoms according to the Saha equation:

$$K_i = [M^+][e^-]/[M]$$

Where K_i is the equilibrium constant, with $[M^+]$, $[e^-]$ and $[M]$ are the concentrations of ions, electrons and neutral atoms, respectively.

4) A dissociation of the molecular species according to the law of mass action. For example, for the reaction $A + B \leftrightarrow AB$ one has:

$$K_p = [A][B]/[AB]$$

In which K_p is the dissociation constant.

5) A density of the radiation between the wavelengths λ and $\lambda+\Delta\lambda$ according to Planck's radiation formula:

$$\rho(\lambda)\, d\lambda = (8\pi hc\, \lambda^{-5})\, [\exp(hc/k\lambda T) - 1]^{-1}\, d\lambda$$

Where c is the velocity of light and h is the Planck constant. Flame gases approach equilibrium in certain aspects, but in other aspects finite differences remain. To answer the question of equilibrium experimentally, many investigators have determined the "formal" temperatures that correspond to different aspects of the system. The better these "temperatures" coincide, the better the state of equilibrium can be assumed to be attained and the more physical meaning the "temperature" of such a system possesses. To avoid confusions the "temperatures" are named after the special process to which they apply , such as translational temperature, excitation temperature, etc. Although there is no *a priori* reason to prefer one "temperature" to another, the translational temperature is often considered the most realistic one, from which the others may deviate. The reason is that the translational energy is very soon equipartitioned (after less than 10 collisions, in approximately 10^{-8} sec at standard pressure). Consequently there is only one translational temperature in one place in the gas. In contrast, to every pair of energy states of every type of particle an excitation temperature (rotational, vibrational or electronic) can be attributed. The number of collisions necessary to attain an equilibrium distribution is approximately 10^3 for rotation, 10^5 for vibration and 10^7 for electronic excitation and dissociation.

Temperature measurements by Boltzmann distribution techniques. In principle any of the equilibrium conditions, mentioned above, could be used to determine the temperature. The foregoing discussion regarding the equilibrium in flames has to be considered when measuring the flame temperature by some emission techniques. All the methods are based on the Boltzmann formula. We recall that the intensity of a spectral line is given by:

$$I = N_n A_n h\nu_n$$

In which A_n is the transition probability of the transition and ν_n is the frequency of the radiation of the spectral line. When no self-absorption occurs by measuring the intensity ratio of two or more spectral lines, the relative populations of the upper levels of these transitions can be obtained by:

$$I_n/I_m = N_n A_n h\nu_n / N_m A_m h\nu_m$$

And by inserting the Boltzmann formula for the population ratio, the working formula becomes:

$$I_n/I_m = (A_n g_n \nu_n / A_m g_m \nu_m) \exp [- (E_n - E_m) / kT]$$

The knowledge of the relative transition probabilities and the measurement of the intensity ratio is sufficient to evaluate the temperature. If E_n and E_m are electronic energy levels of an atom (frequently seeded) within the flame gases, the temperature is an "excitation temperature".

The main sources of error of this method are the uncertainties of the A- values and the occurrence of self-absorption. This latter effect is especially likely to occur when the lower level of the transition is the ground level. Therefore the concentration of the thermometric species should be sufficiently low. Some additional considerations may influence the choice of the pair of lines. The larger the difference between E_n and E_m the more sensitive the intensity ratio is to a change in T, while from a practical standpoint the lines should not be too different either in intensity or in wavelength; this is necessary to avoid cumbersome calibration of the spectrometer and detection system . Some of these requirements are contradictory , but they might be of some help in the choice of the seeding atoms for thermometry and for the measuring lines.

Apart from atomic lines, lines and bands from spectra of naturally occurring molecules have also been used for temperature determination. Due to the fast equilibration of the rotational population, the rotational distribution of diatomic molecules has been frequently measured to infer a "rotational temperature". In this case, the number of spectral lines available partly makes up for the poor precision that one would expect due to the small energy difference between the upper levels of the transitions. Fig. 16 shows the R_1 and R_2 branches of an high resolution rotational spectrum of OH around the band head at 306.4 nm.

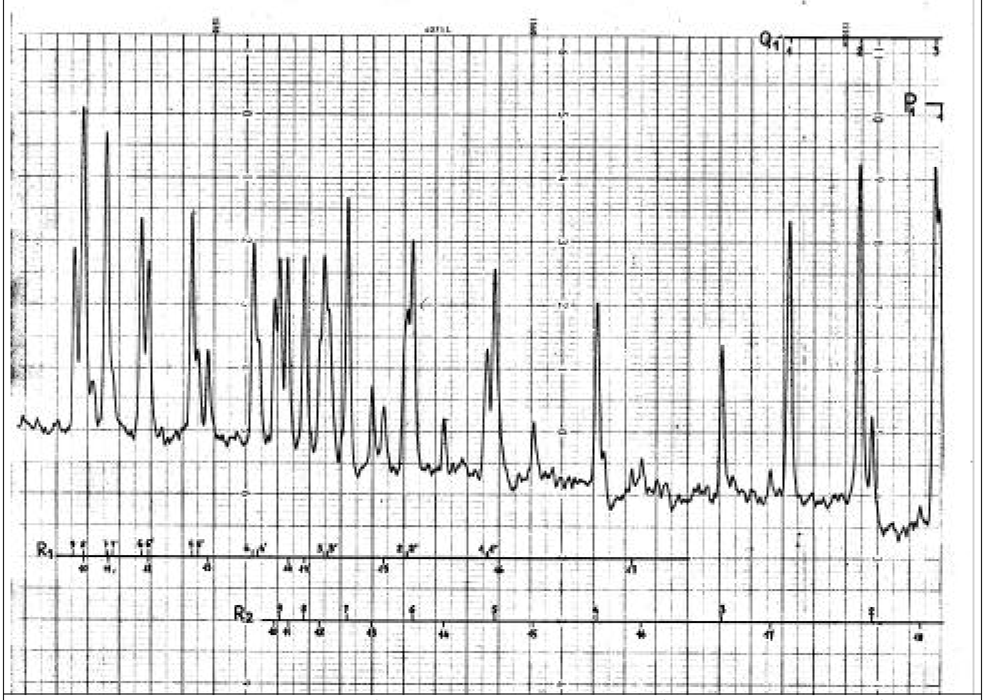

Figure 16. Laboratory chart record of a high resolution spectrum of OH in a methane-air flame. R_1 and R_2 branches of the (0,0) band at 306.4 nm.

In most cases the transition probabilities are not very well known, but the relative transition probabilities of the rotational part can be calculated, while the vibrational and electronic part are equal (in first approximation) for all transitions in the band. The expression for the intensity of the lines in a band can be expressed:

$$I = a\, A_{rot}\, \nu^4 \exp[-E/kT]$$

In which a is a constant A_{rot} is also called the rotational transition probability (but better "strength"), and E is the energy of the rotational level. A plot of (log I- log $A_{rot}\, \nu^4$) versus E yields a straight line of slope –1/kT if equilibrium prevails within the band. Fig. 17 shows a typical laboratory working sheet used to extract the flame temperature (2010 K in this case). The data of Dieke and Crosswhite (1962) are used for the analysis of the rotational spectrum such as the one of in fig. 16. It can be observed that a rather good equilibrium is attained among the rotational levels and that the lines belonging to low rotational quantum numbers are partially self-absorbed, as seen by the fact that the relative points lay below the straight line of the Boltzmann disribution.

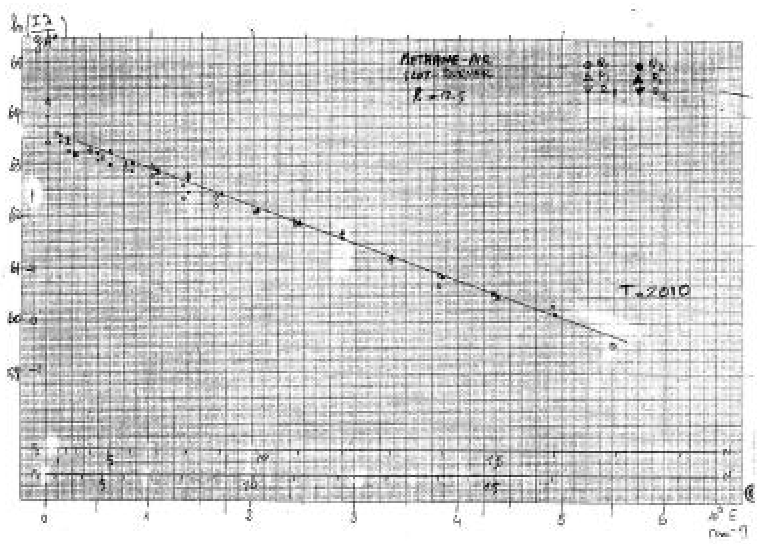

Figure 17. Laboratory sheet for the rotational temperature determination of OH.

The vibrational temperature is obtained in a similar way, by comparing the intensities of a sequence of bands in a molecular spectrum. The intensity of the band can be measured using either the band head or the total profile.

The Line Reversal Method. A different way to obtain electronic excitation temperatures is the Line Reversal method. Instead of using the intensity of two or more emission lines of an atom or a molecule, it is possible to employ the comparison of emitted and absorbed light pertaining to the same transition between two energy levels. One advantage is that, instead of the ratio of the transition probabilities of emission lines, the method is based on the principle of detailed balance, which states that in equilibrium the number of downward radiative transitions should be equal to the number of upward radiative transitions. If the flame contains atoms emitting a radiation of frequency $\nu = (E_i - E_j)/h$ with respective populations of the levels N_i and N_j per unit volume, the reversal of the line occurs when the intensity of the black body radiation at a temperature T_r is such that the part which is absorbed by the atoms is exactly compensated by their emission. For simplicity let us assume that a black body surrounds the flame, so it generates a spectral volume density of radiant energy $\rho(\nu, T_r)$. At the reversal condition the number of photons absorbed and emitted by spontaneous and stimulated emissions are given by:

$$A_{ij} N_i + B_{ij} \rho(\nu, T_r) N_i = B_{ji} \rho(\nu, T_r) N_j$$

By replacing $\rho(\nu, T_r)$ by the Plank equation and by using the fundamental relationships for the Einstein transition probabilities, it is easy to derive:

$$N_i / N_j = g_i / g_j \exp [- (E_i - E_j) / kT_r]$$

If the atoms are in thermodynamic equilibrium at the flame temperature, T, the Boltzmann law holds:

$$N_i / N_j = g_i / g_j \exp [- (E_i – E_j) / kT]$$

Identification of these expressions leads to $T = T_r$. The temperature determined in such a way is an “electronic excitation” temperature.

The method is a “null” method. If the flame temperature is lower that the black body temperature, an absorption line is observed, an emission line is observed in the opposite case. Exact balancing of the black body emission allows a very accurate determination of the flame temperature. There are several advantages connected with this method. The intensities of both emission and absorption lines are affected by self-absorption in exactly the same way. The ratio N_i /N_j is involved and is constant at a constant temperature, therefore reversal temperatures do not depend on the concentration of the thermometric species. The major disadvantage consists in the need of a calibrated source with a brightness temperature at least equal to the flame temperature, (although some 500 K higher temperatures can be measured with an extrapolation procedure).

The technique is practically performed as follows. An image of a reference light source is formed in the flame, and a second image of the reference light source and the flame is formed on the slit of a spectrograph (figure 18).

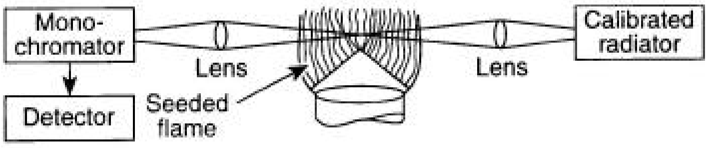

Figure 18. Experimental arrangement for the Line Reversal technique.

Generally a salt (sodium, lithium, iodine, etc.) is introduced into the flame to “color” the flame and generate the spectral line. The band of OH at 306.4 nm has been used sometimes. The most used reference source is the tungsten strip lamp, that must be calibrated in terms of radiation temperature at a certain wavelength versus current. Corrections for tungsten emissivity, lens and optical surfaces losses must be introduced. Tungsten strip lamps can be used up to about 2500 K radiation temperature. The adjustment to the “reversal point” is made by varying the intensity of the image of the lamp within the flame until neither an emission line nor an absorption line is observed in the spectrum (figure 19).

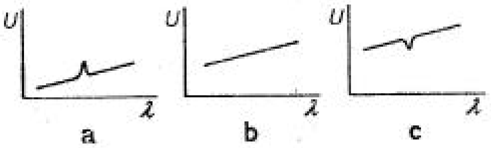

Figure 19. The spectral distribution of the radiation from a source emitting a continuous spectrum, as seen through a layer of gas that emits and absorbs radiation in a spectral line, for various values (a low, c high) of the brightness temperature of the source

Practical considerations and thorough discussions about sources of errors and precision of the Line Reversal technique can be found in the following papers (Snelleman *et alii*, 1968), (Strong *et alii*, 1954), (Strong *et alii*,), (Daily *et alii*, 1976), (Lapworth, 1974).

Apart from laboratory flames temperature measurements, several practical applications of the technique involved measurements in shock tubes for high temperature chemistry (Gaydon *et alii*, 1962), (Clouston *et alii*, 1958), in internal combustion engines (Smith *et alii*, 1969) and at the exit of small rockets (Griggs *et alii*, 1966)

Industrial combustion monitoring and control

Emission spectroscopy in the UV region, in general, does not allow quantitative measurements in flames due to the lack of thermal equilibrium in the population of different excited molecular states. Several laser techniques have been developed for combustion diagnostics. In particular, laser absorption methods, which allow real quantitative results in temperature and concentrations measurements, have almost completely replaced the emission spectroscopy techniques for combustion monitoring . On the other hand emission spectroscopy can be very easily used for flame monitoring as it requires merely a lens and a spectrometer. Recently emission techniques have been rejuvenated and many papers appeared in literature to propose these technique for the active combustion control in several industrial environments.

UV-VIS emission spectroscopy and tomography. A sensor system has been developed which is based on UV emission spectroscopy in combination with tomographic evaluation (Obertacke *et alii*,. 1996). The sensor system contains in a case the imaging optics, with a detection angle of 90 degrees, a spectrometer and a CCD array. The spatial image is projected horizontally and the spectral information vertically on the CCD. Using two sensors simultaneously (figure 20) together with a special tomographic reconstruction algoritm, local intensity values can be achieved. From the spectra the spatial detection of six different molecular species and the local temperature distribution can be obtained. Figure 21 shows, as an example, the emission spectrum of a butane diffusion flame containing contributions of flame radicals and soot black body radiation.

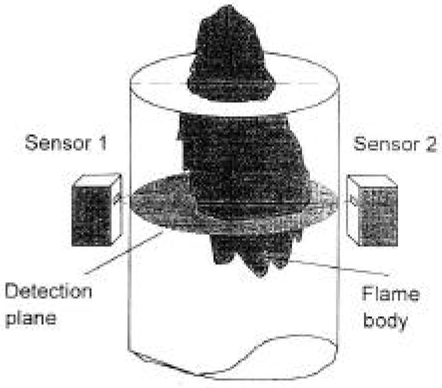

Figure 20. Position of two sensors and detection plane (from Obertacke *et alii*, 1996).

The sensor system has been tested in several industrial environments such as an incinerator and a brown-coal fired combustor for monitoring the combustion processes. Th fast response of the UV band emission stressed the feasibility of an effective control of the combustion processes. Unfortunately the combustion processes are highly non-linear and the evaluation of the spectral information resulted to be very complex forcing the development of particular strategies such as using neural networks and fuzzy tools.

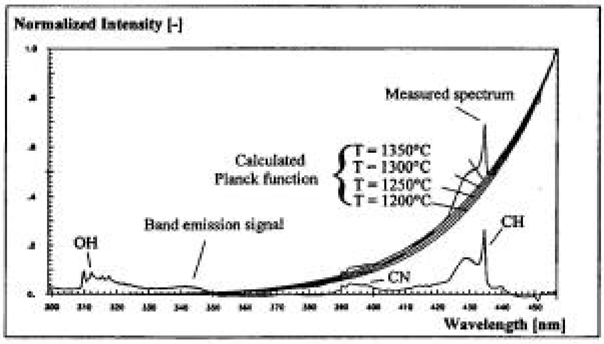

Figure 21. Emission spectrum of a butane diffusion flame containing contributions of flame radical band emissions and soot black body radiation. Also displayed are the calculated Planck functions for different temperatures (from Obertacke *et alii*, 1996)

On this line of research, active combustion control has been demonstrated in oxy-fuel burners (Von Drasek *et alii*, 1998). The sensors are integrated into the industrial burner and are capable of withstanding harsh environment. Radiation from the flame at selected wavelength regions is collected by fiber optics attached to the burner and transported to a miniaturized PC-based spectrometer (figure 22). The spectral information obtained is used to construct a neural network (NN) model that relates the real-time signal to burner operating parameters such as stoichiometry, power and fuel or oxidizer changes (figure 23). This process information from the NN can then be used in a control-loop for adjusting and optimizing combustion parameters or alerting operators of potential burner problems.

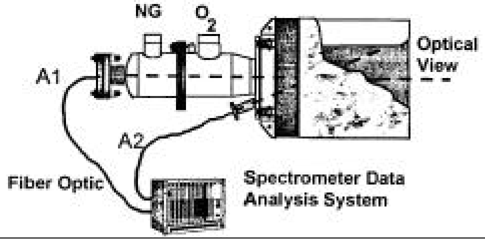

Figure 22. Schematic of the burner adapted for flame emission monitoring at two locations using optical fibers (from Van Drasek *et alii*, 1998).

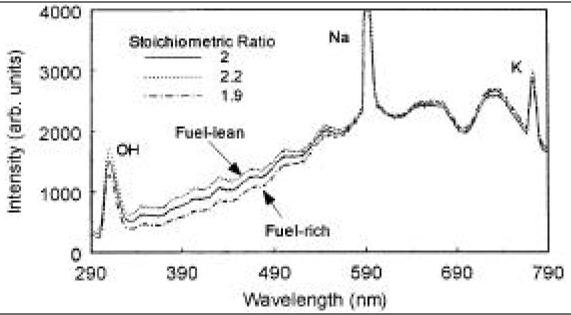

Figure 23. Oxy-fuel flame emission spectra for different stoichiometric ratios at constant power of 350 kW (from Van Drasek *et alii*, 1998)

Air-ratio determination and control in a gas boiler. The installation of multi-port burners in premix-type gas boilers enabled the development of furnaces of compact design. These boilers show an improved thermal efficiency, with the environmental friendly effects of NOx and CO reduction. A simple fiber optic sensor has been developed in order to detect the air-ratio in this type of gas boiler by monitoring the color of the flame and radical emissions. The design and construction of the sensor is simple and suitable for the burner used. Figure 24 shows part of the multi-port plate and the position of the optical fiber. The optical features and spectral characteristics of the flame (figure 25) were analyzed, from which the general specifications for the air-ratio feedback control were derived (figure 26). The control system had been shown to be able to maintain the combustion conditions of an actual burner, with the advantages of both low environmental pollution and high thermal efficiency.

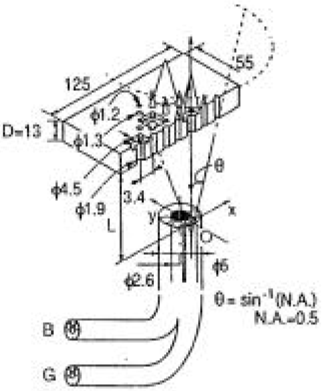

Figure 24. Dimensions of the multi-port burner and details of the sensor head (from Yamaguchi *et alii*, 1997).

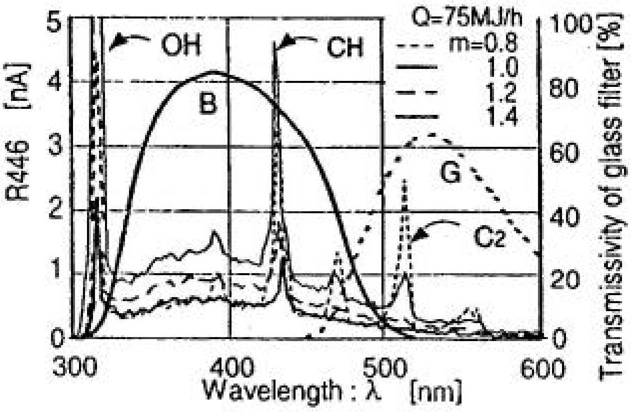

Figure 25. Intensity of radical emissions and relationship with the air-ratio, m. (from Yamaguchi *et alii*, 1997)

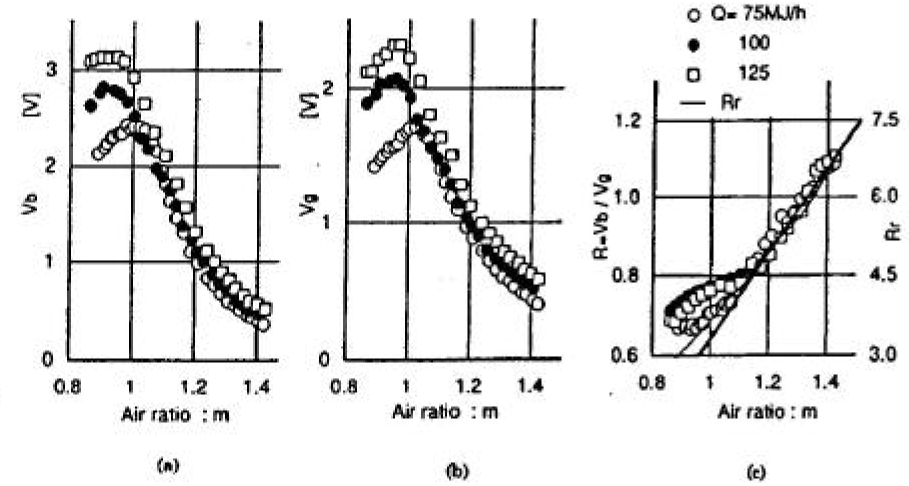

Figure26. Relationship between the air-ratio, m, and the signals of CH (Vb), C2 (Vg) and their ratio, R, (from Yamaguchi *et alii*, 1997)

References

Alkemade, C.Th.J., Herrmann, R., (1979), *Fundamentals of Analytical Flame Spectroscopy*, Hilger, Bristol, UK.

Clouston, J.G., Gaydon, A.G., Glass, I.I., (1958); Temperature measurements of shock waves by spectrum-line reversal method, *Proc.Roy.Soc.*, **248**, 429-444.

Daily, J.W., Kruger, C.H., (1976), Effects of cold boundary layers on spectroscopic temperature measurements in combustion gas flows, *AIAA paper 76-134.*

Dieke, G.H., Crosswhite, H.M., (1962); The ultraviolet bands of OH, *J. Quant. Spectrosc. Radiat. Transfer*, **2**, 97-199.

Gaydon, A.G., (1957); *The Spectroscopy of Flames*, Chapman and Hall, London.

Gaydon, A.G., Hurle, I.R. (1962), Measurements of times of vibrational relaxation and dissociation behind shock waves in N_2, O_2, air, Co, CO_2 and H_2, *8th Symposium on Combustion*, 309-318, The Combustion Institute

Griggs, M., Harlshbarger, F.C., (1966); Measurements of temperature profiles at the exit of small rockets, *Appl.Opt.*, **5**, (2), 211-214.

Guillaume, P., VanTiggelen, P.J., (1984); Spectroscopic investigation of acetylene-nitrous oxide flames, *20th Symposium on Combustion*, The Combustion Institute, Pittsburgh, PA, pp. 751-760.

Lapworth, K.C., (1974); Spectroscopic temperature measurements in high temperature gases and plasmas, *J.Phys.E: Sci.Instrum.*, **7**,413-420.

Mavrodineanu, R., Boiteux, H., (1965); *Flame Spectroscopy*, Wiley, New York.

Najim, H.N., Paul, P.H., Mueller, C.j., Wyckoff, P.S., (1998), On the adequacy of certain experimental observables as measurements of flame burning rate, *Comb.Flame*, **113**, 312-332,

Obertacke, R., Wintrich, H., Wintrich, F., Leipertz, A.(1996); A new sensor system for industrial combustion monitoring and control using UV emission spectroscopy and tomography, *Comb.Sci.and Technol.*, **121**, 133-151.

Porter, R.P., Clark, A.H., Kaskan, W.E., Browne, W.E., (1966); A study of hydrocarbon flames, *11th Symposium on Combustion*, The Combustion Institute, Pittsburgh, PA, pp. 907-917.

Pungor, E., Cornides, I.; (1969), Emission problems of unsalted flames, in *Flame Emission and Atomic Absorption Spectrometry – Vol. 1*, J.A. Dean and Th. C. Rains Ed.s, Dekker, London, UK.

Smith, D.S., Starkman, E.S., (1969); Spectroscopic method for simultaneous determination of species concentration and temperature in a cyclic combustion process, *Rew.Sci.Instrum.*, **40**, (12), 1541-154.

Snelleman, W., Smith, J.A., (1968); A flame as a secondary standard of temperature, *Metrologia*, **4**, (3), 122-134

Strong, H.M., Bumdy, F.P., (1954); Measurement of temperatures in flames of complex structure by resonance line radiation. I. General theory and application to sodium line reversal methods, *J.Appl.Phys.*, **25**, (12), 1521-1526.

Strong, H.M., Bundy, F.P., Larson, D.A.; (Temperature Measurement on complex flames by sodium line reversal and sodium D line intensity contour studies, *Third Symposium on Combustion*, 641-647.

Von Drasek, W., Charon, O., Marsais, O., (1998), Industrial combustion monitoring using optical sensors; *SPIE Meeting on Industrial and Environmental Monitors and Biosensors*, Boston, Nov. 2-5.

Wohl, K., Welty, F., (1955); Spectrophotometric traverses through flame fronts, *5th Symposium on Combustion*, The Combustion Institute, PA. pp. 746-753.